Insight into the role of TXNRD2 in steroidogenesis through a novel homozygous *TXNRD2* splice variant

Cécile Brachet[1]*, Alexander Laemmle[2,3,4]*, Martine Cools[5], Kay-Sara Sauter[2,3], Elfride De Baere[6], Arnaud Vanlander[7], Amit V. Pandey[2,3], Therina du Toit[3,8], Clarissa D. Voegel[3,8], Claudine Heinrichs[1], Hannah Verdin[6#], Christa E. Flück[2,3#]

*: shared first authors

#: shared senior authors

[1] Université libre de Bruxelles (ULB), Hôpital Universitaire de Bruxelles (H.U.B), Hôpital Universitaire des Enfants Reine Fabiola (HUDERF), Paediatric Endocrinology Unit, Avenue J.J. Crocq 15 1020 Bruxelles, Belgium

[2] Division of Pediatric Endocrinology, Diabetology and Metabolism, Department of Pediatrics, Inselspital, Bern University Hospital, University of Bern, 3010 Bern, Switzerland

[3] Department of Biomedical Research, University of Bern, 3010 Bern, Switzerland

[4] Institute of Clinical Chemistry, University of Bern, 3010 Bern, Switzerland

[5] Department of Internal Medicine and Pediatrics, Ghent University; Department of Pediatrics, Division of Pediatric Endocrinology, Ghent University Hospital, Ghent, Belgium

[6] Center for Medical Genetics, Ghent University Hospital; Department of Biomolecular Medicine, Ghent University, C. Heymanslaan 10, 9000 Gent, Belgium.

[7] Mitochondrial Investigations Laboratory, Ghent University C. Heymanslaan 10, 9000 Gent, Ghent, Belgium and Department of Internal Medicine and Paediatrics, Ghent University Hospital, Ghent, Belgium

[8] Department of Nephrology and Hypertension, Inselspital, Bern University Hospital, University of Bern, 3010 Bern, Switzerland

Corresponding Author:

Christa E. Flück

University Children's Hospital Bern

Freiburgstrasse 65 / C845

3010 Bern

Switzerland

christa.flueck@unibe.ch

ORCID 0000-0002-4568-5504

Short title (44/46): Impact of variant *TXNRD2* on steroidogenesis

Key words: TXNRD2, primary adrenal insufficiency, gonadal insufficiency, steroidogenesis, mitochondrial reactive oxygen species

Word counts: Text 3862/3500

Abstract (230/250)

Objective. Adrenal cortisol production occurs through a biosynthetic pathway which depend on NADH and NADPH for energy supply. The mitochondrial respiratory chain and the reactive oxygen species (ROS) detoxification system are therefore important for steroidogenesis. Mitochondrial dysfunction leading to oxidative stress has been implicated in the pathogenesis of several adrenal conditions. Nonetheless, only very few patients with variants in one gene of the ROS detoxification system, Thioredoxin Reductase 2 (*TXNRD2*), have been described with variable phenotypes.

Design. Clinical, genetic, structural and functional characterization of a novel, bi-allelic *TXNRD2* splice variant.

Methods. On human biomaterial, we performed whole exome sequencing to identify and RNA analysis to characterize the specific *TXNRD2* splice variant. Amino acid conservation analysis and protein structure modeling were performed *in silico*. Using patient's fibroblast-derived human induced pluripotent stem cells, we generated adrenal-like cells (iALC) to study the impact of wild-type (WT) and mutant TXNRD2 on adrenal steroidogenesis and ROS production.

Results. The patient had a complex phenotype of primary adrenal insufficiency (PAI), combined with genital, ophthalmological and neurological features. He carried a homozygous splice variant c.1348-1G>T in *TXNRD2* which leads to a shorter protein lacking the C-terminus and thereby affecting homodimerization and FAD binding. Patient-derived iALC showed loss of cortisol production with overall diminished adrenal steroidogenesis, while ROS production was significantly increased.

Conclusion. Lack of TXNRD2 activity for mitochondrial ROS detoxification affects adrenal steroidogenesis and predominantly cortisol production.

Significance Statement (113/120)

Mitochondrial dysfunction leading to oxidative stress has been implicated in the pathogenesis of several adrenal conditions and also in numerous inherited neurodegenerative disorders. Only three families with *TXNRD2* biallelic variants and primary adrenal insufficiency have been published. We report on a patient with primary adrenal insufficiency, hypovirilization, optic neuropathy and spasticity. He harbors a homozygous variant c.1348-1G>T in *TXNRD2*. Its impact on protein structure and function is documented. We show an increased ROS production, loss of cortisol production with decreased adrenal steroidogenesis explaining the combined adrenal and gonadal phenotype of the patient.

This report illustrates the importance of the mitochondrial ROS detoxification system for steroidogenesis along with the phenotypic variability typical of mitochondrial dysfunction.

Introduction

Genetic forms of primary adrenal insufficiency (PAI) may manifest with an isolated steroid disorder phenotype or may be part of more complex syndromes. Pathogenic variants in several genes cause PAI and can be grouped into steroid biosynthesis, cholesterol synthesis, and peroxisomal defects, mitochondrial diseases (due to mitochondrial DNA loss-of function variants or mitochondrial reactive oxygen species [ROS] detoxification defects), DNA-repair defects, autoimmune diseases, ACTH resistance syndromes, adrenal dysgenesis, and others. **(1–4)** Common to all is the typical biochemical finding of cortisol deficiency with elevated adrenocorticotropic hormone (ACTH). When cortisol deficiency is the leading steroid hormone deficiency, conditions are also called ACTH resistance syndromes or familial glucocorticoid deficiency (FGD).

Oxidative stress has been implicated in the pathogenesis of numerous adrenal conditions including adrenoleukodystrophy, **(5)** Triple A syndrome **(6)**, nicotinamide nucleotide transhydrogenase (NNT), **(7)** thioredoxin reductase 2 (TXNRD2), **(8)** and sphingosine-1-phosphate lyase (SGPL1) **(9)** defects, and rarely mitochondriopathies. **(10)**

The mitochondrial ROS detoxification system includes the thioredoxin-peroxiredoxin and glutathione systems. Peroxiredoxin 3 (PRDX3), a peroxidase, is one of the major H_2O_2 scavenging enzymes in the mitochondria. **(11–13)** Both the thioredoxin-peroxiredoxin and the glutathione systems require high concentrations of NADPH which are provided by NNT, located in the inner mitochondrial membrane (**Figure 1**).

Since 2012, several patients and families with biallelic variants in *NNT* and FGD have been reported. **(14,15)** By contrast, only few patients with variants in other genes of this mitochondrial ROS balancing system (e.g. *TXNRD2, TXN2, PRDX3*) have been reported, among which only three index cases with *TXNRD2* variants had an adrenal phenotype (**Table 1**).

The first time that patients with *TXNRD2* monoallelic variants were described was in 2011 when Sibbing et al. reported two novel variants (p.Ala59Thr and p.Gly375Arg) in three heterozygous carriers identified in a cohort of 227 patients with dilated cardiomyopathy (DCM). These patients had no adrenal phenotype. Their reduced ROS scavenging was explained by a dominant-negative effect exerted by mutant TXNRD2 proteins. (16) Similarly, a heterozygous *TXNRD2* variant (p.Pro352Thr) was found in a mother and child where the mother showed severe preeclampsia and was later found to have DCM, while the baby boy was born premature, showed DCM at birth, and died from complications at 5 months of age. (17) Again, no adrenal phenotype was described in these patients. Interestingly, cardiac-specific *Txnrd2* knockout mice also show dilated cardiomyopathy and a thinner ventricular cell wall.

In 2014, Prasad et al. reported seven members of a consanguineous family homozygous for the p.Tyr447* *TXNRD2* variant with FGD and a wide variability in age at diagnosis (one of them (still) not showing FGD at the age of 7.4 years). None presented cardiomyopathy, but one presented with a common truncus arteriosus (**Table 1**) and no other organ dysfunctions were reported. (8) Meanwhile, two additional, unrelated patients with homozygous *TXNRD2* variants have been reported. A biallelic p.(Arg418*) variant was identified in a male patient who manifested at birth with dysmorphic features, omphalocele and hypoglycemia, and was later diagnosed with neurocognitive impairment and glucocorticoid deficiency. (18) More recently, a homozygous p.Val361Met variant was found in a boy manifesting with PAI at 10 years of age who was diagnosed at birth with a micropenis and undescended testis. (19) Thus, many questions remain unsolved concerning the broad variability of phenotypes observed with human variants in genes involved in the mitochondrial ROS detoxification system. While *NNT* variants seem to affect adrenal function predominantly, (15) variants in *TXN2* (20) and *PRDX3* (21,22) are reported in patients with cerebellar ataxia without adrenal dysfunction. Of note, studies have shown that mouse and human differ in tolerance to the loss of selenoprotein function such as thioredoxin reductases or glutathione peroxidases, (23) suggesting that (some) results from mice models might not translate to humans. For instance, loss of *Txnrd2* in mice is embryonically lethal, but may be tolerated in humans.

The aim of this study was to describe the clinical and genetic findings of a patient with a novel *TXNRD2* splice variant, and to study its specific impact on adrenal steroidogenesis by modeling adrenal function using patient-derived, induced pluripotent stem cells (iPSC) that were differentiated into adrenal-like cells (iALC).

Materials and Methods

Written informed consent was obtained from the patient and his parents for DNA analysis, skin biopsy, fibroblast culture and case report publication. Clinical data were extracted from the hospital file retrospectively and pseudoanonymized. The study was approved by the independent ethics committee of Ghent University (ref 2008/098 BC-5963) and conducted in compliance with the Declaration of Helsinki.

Genetic workup

Chromosome analysis revealed a normal male karyotype without any visible numerical or structural aberrations. Mosaicism was excluded by fluorescence *in situ* hybridization (FISH). Whole exome sequencing (WES) and analysis revealed a homozygous splice site variant in the *TXNRD2* gene (NM_006440.3): c.1348-1G>T (**Suppl Material**). Segregation analysis in the parents and unaffected sister was performed with Sanger sequencing.

cDNA analysis

For cDNA analysis, total RNA was extracted from short-term cultured lymphocytes treated with or without puromycin using MagCore according to the manufacturer's guidelines. cDNA was synthesized with the iScript cDNA Synthesis Kit (Bio-Rad Laboratories). PCR amplification was performed using primers F-CACGCCCATTATAAACCACTGG and R-ATGGCGCTTACCCTCAGC. PCR products were assessed by direct sequencing.

Structural analysis

Amino acid sequences from the NCBI database were used for amino acid conservation analysis (**Suppl Material**). A three-dimensional structural model was made by homology modeling using the structures of mouse thioredoxin reductase type 2 (PDB# 3DGZ) and rat thioredoxin reductase type 1 (PDB# 4KPR) X-ray crystal structures which were selected based on a Phi-BLAST search of the amino acid sequences derived from the PDB structure database. Then a secondary structure prediction was performed to aid in alignment correction and loop modeling by running a PSI-BLAST to create a target sequence profile and feeding it to PSI-PRED secondary structure prediction program. Models were then generated as a homodimer based on alignments to templates. The best parts of models were combined to create a final hybrid model that covered the maximum sequence of the human TXNRD2 protein. The model was refined by molecular dynamics simulations using AMBER force field under YASARA. The model of the mutant protein was constructed in a similar way, starting from scratch to simulate the natural protein production and folding.

Fibroblast culturing

The patient´s fibroblasts were cultured from a skin biopsy. Established cell cultures were stored in liquid nitrogen until further use.

Patient-derived iPSC generation and differentiation into iALC

Patient-derived iPSCs were generated from the patient's fibroblasts and cultured as previously described (24). Healthy control iPSC were available from other projects. (25) (26) Differentiation of iPSC into iALC was performed for both healthy controls and *TXNRD2* variant cells according to the protocol of Li et al. (27) In brief, after about 6 weeks, expression of essential genes of steroidogenesis was confirmed by RT-PCR. For each reprogrammed iPSC line, differentiation into iALC was performed in parallel lineages, 5-times. The genetic background of the WT and variant *TXNRD2* was confirmed by Sanger sequencing (Microsynth).

RNA analysis for assessment of splicing of TXNRD2

RNA was extracted from WT *TXNRD2* and c.1348-1G>T variant iALC. Reverse transcription and PCR amplification was performed using primers F-tctatcacgcccattataaaccact and R-accctcagcagcctgtcaccgt. PCR products were assessed by direct sequencing.

Steroid profiling

For steroid profiling, final iALC cultures received fresh medium for 24 hours before steroid metabolites secreted into the supernatants were collected and stored at -20°C. Steroid analysis was performed by an in-house liquid chromatography-high resolution mass spectrometry (LC-MS) method as previously described. (28) Data from the mass spectrometer was processed using TraceFinder 4.0.

MitoSOX-Based Flow Cytometry

On day 26 of iALC differentiation, production of ROS was measured by a MitoSOX Red-based fluorescence assay (Invitrogen) on a flow cytometer (**Suppl Material**).

Statistics

All experiments were repeated at least three times with a minimum of two biological replicates. Student *t*-test or two-way ANOVA was used to compare groups, with significance at $p < 0.05$. Data are expressed as mean and SEM. For calculations and graphs GraphPad Prism 9 was used (GraphPad ware Inc., San Diego, CA).

Results

The index case is the third child of highly consanguineous parents of Moroccan origin: grandmothers are sisters and grandfathers are brothers (**Figure 2A**). By history, four siblings of the mother died in early infancy in Morocco (no investigations). She also had herself two early and one late stillbirth at 28 weeks gestation (normal male fetus, no investigations). The index case was born at term after an uneventful spontaneous pregnancy with a birth weight of 3170 g, a birth length of 48 cm and head circumference of 34.5 cm. Micropenis (SPL 1cm) with bilateral scrotal testes, without hypospadias were noted at birth. He presented a mild hypoglycemia during the first 24 hours of life and a mild jaundice. Karyotype was 46,XY, no evidence for testicular dysgenesis was found (normal AMH, no Mullerian remnants), testosterone was low, including after hCG stimulation test (**Table 2**).

At 21 months, he presented with seizures during a viral infection and was found to be hyperpigmented. He was diagnosed with PAI (Table 2) and started on replacement therapy

with hydrocortisone and 9-alpha-fludrocortisone (12 mg/m^2/d and 50 µg/d, respectively). In retrospect, ACTH was already elevated at 4 months. Other causes of PAI were excluded. Concerning psychomotor development and neurology, the child developed normally until the age of 6-12 months, when gradual spastic diplegia was noted. He could walk independently at 3 years and talk in phrases at 4 years of age. His spastic diplegia required physiotherapy, splints wearing, wheelchair even for short journeys. His language and cognitive capabilities were spared compared to his motor skills and he could write and read with a computer (given his low vision, see below). Brain MRI at 2 years of age showed a white matter signal abnormality especially marked in the corpus callosum and the heads of the caudate nuclei and anterior side of the putamen associated with a lactate peak on spectroscopy, suggesting a metabolic cause. In addition, the choroidal plexuses was reported to have a globular appearance with a cystic component. The spectroscopic signal abnormalities were stable over time at a follow-up MRI at 14 years of age.

Ophthalmological examination showed low vision from the age of 5 years with optic neuropathy confirmed by OCT (optical coherence tomography) at the age of 11 years (visual acuity 1/02 and 1/10, photophobia and low color vision). Formal hearing assessment was normal at 12 years of age (including Brainstem Auditory Evoked Potentials).

With respect to postnatal sexual development, he underwent a left scrotal surgical exploration for an acute scrotum at 13 months of age. The left testis was slightly high in the scrotum, but of normal appearance. At 12 years of age, he entered spontaneous puberty with an increase in testicular volume and testosterone showing pubertal serum levels at 13 years of age. However, at 16 years of age, with a pubertal Tanner stage G4, P4 and testes volumes of 12 mL/12 mL, penile length of 6.5 cm, a relative testicular insufficiency was observed with elevated gonadotropins, but testosterone still within normal range. No other endocrinopathies were noted. Cardiac ultrasound was normal at 13 years of age. Heterozygous parents were healthy without any cardiac, endocrine, or neurological phenotype.

WES revealed a homozygous *TXNRD2* splice acceptor variant, c.1348-1G>T, both parents and the unaffected sister were heterozygous carriers (**Figure 2**). The variant is not present in the population database gnomAD v4.0.0 and several prediction tools (SpliceAI, ADA, MaxEntScan) predicted a loss of the acceptor splice site. To assess the effect on splicing, cDNA analysis on patient fibroblasts was performed. This showed that the *TXNRD2* c.1348-1G>T variant caused a splicing error and resulted in exon 16 skipping which is predicted to result in a frameshift p.(Met450Valfs*20). The new stop codon is located within the last 50 base pairs of the penultimate exon; the truncated transcript is predicted to escape nonsense-

mediated decay leading to a shorter protein product. The latter could be confirmed as samples treated with or without puromycin led to the same result (**Figure 2B**).

We made a three-dimensional structural model of the WT and p.(Met450Valfs*20) versions of the proteins to analyze the effect of the mutant protein on structure and function. A multiple sequence alignment of TXNRD2 homologues across species showed a highly conserved C-terminus (**Figure 3A and Suppl Figure 1**). Analysis of the monomeric forms of the WT (**Figure 3B**) and mutant structures (**Figure 3C**) showed that the mutant protein can still form a partial structure but has several missing residues at the C-terminus (**Figure 3D**). The WT TXNRD2 exists as a homodimer with C-terminus residues of both subunits of the dimer contributing towards dimer formation (**Figure 3E** and **Suppl Figure 2**). Dimerisation has been shown essential for the enzymatic activity of TXNRD2. An active site selenocysteine located at the dimer interface, is encoded by a TGA/UGA codon and is present in the human WT protein (**Figure 3F**) but may be missing in many automated computer derived annotations due to being falsely assigned as a stop codon (**Suppl Figure 1**). In addition, His 461 (Histidine 497 in the full length protein) residues of each monomer are involved in the binding of FAD from the other monomer of the dimeric structure (**Suppl Figure 3**). Based on the effect of missing C-terminus residues involved in dimer formation and FAD binding we conclude the mutant to be devoid of enzyme activity.

To study the impact of the *TXNRD2* c.1348-1G>T variant on steroidogenesis specifically, we used patient-derived iPSC (reprogrammed from skin fibroblasts) and differentiated them into iALC. (27) These cells were confirmed to show the genetic background of our patient, compared to the WT-derived control iALC (**Figure 2C**). Reverse transcription analysis of RNA extracted from these iALC showed that the *TXNRD2* c.1348-1G>T variant caused a splicing error and resulted in exon 16 skipping leading to a shorter protein product of 469 instead of 541 amino acids (**Figure 2D**).

Steroid profiles of the WT and variant iALC lines were then assessed by high-resolution mass spectrometry (28) and revealed that the *TXNRD2* variant lines produced significantly less steroids comprised in all three steroid pathways (**Figure 4**). It affected the glucocorticoid (GC) path most, followed by the mineralocorticoid (MC) path, and the adrenal androgens (**Figure 4A**). Thus, compared to control iALC, the variant iALC revealed no cortisol production, and less aldosterone, DHEA and testosterone production (**Figure 4B**). Pregnenolone, the first and rate-limiting steroid metabolite produced from cholesterol in mitochondria that is needed as precursor for all steroid paths, was also grossly reduced.

As TXNRD2 is involved in the network for maintaining mitochondrial ROS balance, we also tested the WT and variant iALC for ROS/superoxide production using MitoSOX Red-based flow cytometry. (29)This experiment showed that the *TXNRD2* c.1348-1G>T iALC lines produced significantly higher levels of ROS/superoxide compared to control cell lines indicating disrupted ROS detoxification (**Figure 5A, B**). Quantification of H_2O_2 production using the MitoSOX probe showed a 20-fold increase for WT iALC compared to a 52-fold increase for variant iALC (**Figure 5C**).

Discussion

We report on a patient with PAI, micropenis, white matter brain disease, and optic neuropathy who was found to carry a novel homozygous splice acceptor variant, c.1348-1G>T, in the *TXNRD2* gene leading to exon 16 skipping and p.(Met450Valfs*20). Both PAI and optic neuropathy appeared over time with PAI manifesting at age 21 months triggered by an infection. His parents were healthy carriers. Our report is the first to provide insight into the functional impact of TXNRD2 on adrenal steroidogenesis specifically. Table 1 summarizes characteristics of three previously reported families with biallelic *TXNRD2* variants. The first reported on seven members of a consanguineous family homozygous for the p.Tyr447* TXNRD2 with an almost exclusively adrenal phenotype and exhibiting FGD with wide variability in age at diagnosis. (8) The second report was about a child homozygous for the p.Arg418* variant with developmental delay, syndromic features, neurocognitive impairment, and cortisol deficiency. (18) In the third report, a boy with micropenis and cryptorchidism at birth and isolated GC deficiency at 10 years of age was described who was found to carry homozygous TXNRD2 p.Val361Met. (19) This boy also carried a heterozygous variant of uncertain significance of *CYP11B1* (c.1182C>G/p.Asn394Lys). By contrast, the patients from four unrelated families reported with monoallelic, heterozygous missense *TXNRD2* variants (p.Ala59Thr, p.Gly375Arg, and p.Pro352Thr) were affected by dilated cardiomyopathy only but no FGD. (16,17)

Mammalian thioredoxin reductases (TrxRs) are homodimers, comprised of three domains, including a FAD-binding domain (mTrxR2 residues 35–190, 322–392), an NADPH-binding domain (mTrxR2 residues191–321), and a redox-active interface domain (mTxrR2 residues 393–524). (30) For the catalytic reaction with TXNRD2, the reducing equivalents from NADPH (e.g. oxidized TXN2) are first transferred to FAD, then passed on to the N-terminal redox-reactive center and finally to the Sec-containing C-terminal catalytic site of the second monomer. The reported homozygous TXNRD2 variants p.Tyr447* and p.Arg418* affect the redox-active interface domain and FAD binding, while the missense variants p.Ala59Thr, p.Gly375Arg and p.Pro352Thr (reported in heterozygous state in patients with

cardiomyopathy) are located in the FAD-binding domain. Residues G375 and A59 in FAD domain are highly conserved across a wide range of species. (16) Functional studies of these two identified missense mutants reconstructed in murine fibroblasts showed that both are unable to rescue Txnrd2 -/- cells from cell death induced by glutathione (GSH) depletion and that they exert a dominant-negative effect when expressed in Txnrd2+/+ cells. (16) Based on our structural analysis, a dominant negative effect is expected, since even one copy of the protein with missing C-terminus residues will lack the active site that is formed by contributions of both subunits of the dimer. This will affect overall enzyme function which requires homodimer formation, by competing with the functional copy of the protein and making a non-functional dimeric protein. The conserved C-terminal possesses an essential seleno-cysteine (SeCys/Sec) residue, which is crucial for the catalytic activity of TXNRD2, as its removal leads to complete loss of activity. (Zhong et al. 1998; Zhong, Arnér, and Holmgren 2000; Sandalova et al. 2001) In both p.Tyr447* and p.Arg418* variants reported in homozygous state, the C-terminal end of the protein is lost, explaining the loss of TXNRD2 activity. Similarly, the newly reported p.Met450Valfs*20 severely disrupts dimer formation and FAD binding.

In 2014, Prasad et al. have reported an affected mitochondrial redox homeostasis in *TXNRD2* knockdown of human adrenocortical H295R cells. This was documented by a 3-fold increase in levels of mitochondrial ROS, a decrease in the GSH to GSSH ratio and lower levels of reduced mitochondrial PRDX3. (8) We performed similar experiments in patient-derived iPSC that were differentiated into iALC and confirm the negative impact of the c.1348-1G>T variant in *TXNRD2* on adrenal ROS production. In addition, our study shows for the first time the direct effect of a human *TXNRD2* mutation on adrenal steroidogenesis. Interestingly, we found that cortisol production of the steroid biosynthesis was most severely affected, corresponding to the reported FGD phenotype. However, in our iALC we also observed an impact on pregnenolone production, which informs on an additional – though less severe - effect on the first steps of steroidogenesis (e.g. STAR and CYP11A1 activities) essential for overall steroidogenesis. This might explain the lower aldosterone and DHEA production that we observed in *TXNDR2* mutant iALC (as well as in the patient). Effect of TXNRD2 deficiency on overall steroidogenesis (not only on the adrenal cortex) might explain the genital phenotype observed in our patient (and the recently reported patient by Patjamontri (19)) at birth and the impending testosterone deficiency evidenced by increased LH and FSH at age 17 years (Table 2). Testicular disorders have also been reported in patients with biallelic NNT mutations. (31) (32) As TXNRD2 is widely expressed in various tissues, individuals with TXNRD2 deficiency are at risk of developing extra-adrenal disorders.

Although there is convincing evidence from bioinformatics tools and functional studies for the pathogenicity of the *TXNRD2* variants reported in the literature and in the current study, the broad spectrum of phenotypes remains unexplained. We do not understand why the seven members of the consanguineous family with the TXNRD2 p.Tyr447* variant have an almost exclusively adrenal phenotype, whereas the other patients show additional features including genital anomalies and neurological manifestations (**Table 1**). It also remains unexplained why they have no cardiac manifestations, while individuals with heterozygous *TXNRD2* variants have been described with an isolated cardiac phenotype (DCM). While a dominant negative effect of some TXNRD2 variants (p.Ala59Thr, p.Gly375Arg) has been reported, (16) variable gene expressivity and oligogenicity have been proposed as possible genetic explanations. Potential contribution by other genetic factors might be considered, especially in patients with a consanguineous background. In addition, tolerance to loss of selenoprotein function such as thioredoxin reductases or glutathione peroxidases might not only be species specific, (23) but also tissue specific and even different between individuals. TXNRD2 deficiency might be variably compensated by the glutathione system, which can keep PRDX3 reduced. This hypothesis might be worth addressing in future studies.

The ROS detoxification system does not only depend on TXNRD2 but consists of two parallel cascades: the thioredoxin and glutathione systems which both reduce PRDX3 (**Figure 1**). This cascade requires high concentrations of NADPH from NNT. NADPH molecules are also essential for supporting the catalytic activities of CYP11A1 and CYP11B1/2 enzymes in steroidogenesis. **(33)** However, the electron transfer from NADPH to CYP11A1 (for the production of pregnenolone) has been shown to be more efficient than to CYP11B1 (for cortisol production). **(34)** This probably explains our findings of a predominant inhibition of CYP11B1 activity on the adrenal steroid profile of mutant TXNRD2 iALC.

With the exception of homozygous *NNT* variants found in about 5-10% of FGD patients **(15)** and extremely rare *TXNRD2* variants, **(8,18,19)** no other variants in genes involved in the mitochondrial ROS balancing system have so far been reported with an adrenal phenotype. Rare variants in *TXN2* and *PRDX3* have been described in patients with rather severe neurological phenotypes. In 2016, Holzerova reported a patient with a homozygous *TXN2* variant. **(20)** In mitochondria, TXN2 is reduced by TXNRD2 and NAPDH. H_2O_2 is sensed by PRDX3 and oxidation of PRDX3 is reduced by TXN2. The reported patient with a biallelic stop-gain *TXN2* variant (p.Trp24*) presented with an infantile-onset neurodegenerative disorder with severe microcephaly and fast progressive cerebellar atrophy, drug resistant epilepsy, dystonia, optic atrophy, and peripheral neuropathy. **(20)** The cerebellum appeared to be specifically vulnerable, which was also observed in Txnrd1 nervous system-specific null

mice, while Txnrd2 nervous system-specific null mice developed normally. **(35)** Similarly, biallelic variants in *PRDX3* (the mitochondria specific antioxidant enzyme) were found to cause progressive cerebellar ataxia with concomitant movement disorders, due to severe early-onset cerebellar atrophy, and olivary and brainstem degeneration in six independent individuals. **(21,22)**

In conclusion, we here show the direct impact of a very rare homozygous *TXNRD2* variant on mitochondrial ROS detoxification and adrenal steroidogenesis. Steroid profiling of patient-derived iPSC differentiated into iALC suggests severe disruption of cortisol production (CYP11B1 activity), but also an impact on pregnenolone production (CYP11A1 activity) and thus overall steroidogenesis. This likely explains the combined adrenal and gonadal phenotype of the patient. In addition, the patient has severe optic neuropathy and spastic diplegia due to white matter disease, both classical features of mitochondrial neurodegenerative conditions. The phenotypic variability among reported patients with bi-allelic *TXNRD2* variants, monoallelic variants and variants in other genes of the ROS detoxification system remains a conundrum. Additional genetic factors and tissue-specific tolerance to selenoprotein dysfunction may play a role.

Declaration of conflicts of interest.

The authors have no conflict of interest to declare.

Funding and Acknowledgment

Arnaud Vanlander is supported by Ghent University, special research fund (BOF-Tenure Track, BOF/STA/202209/040).

Data sharing /availability statement. All patient and experimental data are included in the manuscript. Further details may be provided upon reasonable request protecting the patient's and family's anonymity.

Authors' contribution

CB – Clinical investigations, study design, first manuscript draft. ORCID 0000-0001-7955-2534. Email: cecile.brachet@hubruxelles.be

AL – *In vitro* iPSC generation and experiments, manuscript proofing. ORCID 0000-0001-9191-1886. Email: alexander.laemmle@insel.ch

MC – Clinical work-up, study design, manuscript proofing. ORCID: 0000-0002-9552-4899. Email: Martine.cools@ugent.be

KSS – Lab work, *in vitro* experiments, data analysis. Email: kay.sauter@unibe.ch

EDB – Genetic studies. ORCID 0000-0002-5609-6895. Email: elfride.debaere@ugent.be
AV – Clinical studies, genetics, manuscript proofing. ORCID: https://orcid.org/0000-0002-9520-5564. Email: arnaud.vanlander@ugent.be
AVP – Protein bioinformatics. Email: amit@pandeylab.org
TdT – Steroid measurements and analysis. ORCID: orcid.org/0000-0002-3533-0590. Email: therina.dutoit@unibe.ch
CV - Steroid measurements and analysis. Email: clarissa.voegel@unibe.ch
CH – Clinical studies, case report. Manuscript proofing. Email: claudine.heinrichs@hubruxelles.be
HV – Overall design, genetic studies, and analyses. Manuscript proofing. ORCID 0000-0002-0258-1000. Email: hannah.verdin@ugent.be
CEF – Overall design, *in vitro* studies, data analysis, manuscript preparation and final proofing. Study PI and Corresponding author.

Figure Legends

Figure 1. Schematic picture of the ROS defence system in mitochondria. Two parallel cascades are established, the thioredoxin and glutathione systems, to reduce PRDX3. Different proteins and complexes of the oxidative phosphorylation system (OXPHOS) produce ROS in the form of superoxide (O_2^-), which spontaneously, or with the help of manganese superoxide dismutase (MnSOD), converts to hydrogen peroxide (H_2O_2). In the thioredoxin pathway, H_2O_2 is sensed by PRDX3 and oxidation of PRDX3 is reduced by TXN2. TXN2 is reduced by TXNRD2 and NAPDH. In the glutathione pathway, glutathione peroxidase (GPx) reduces H_2O_2 and is reduced by GSH molecules, which form dimers (GSSG) or by glutaredoxin 2 (GLRX2). GSSH dimers are reduced by glutathione reductase (GR) and NADPH.

Figure 2. Genetic findings. A. Family tree. B. *TXNRD2* gene analysis from patient's leukocytes. C, D. Genetic characterization of patient-derived iPSC differentiated into induced adrenal cells (iALC) in comparison to a wild-type (WT) control cells. Direct sequencing of genomic DNA extracted of WT and mutant iALC (C). RNA analysis (RT-PCR) of iALC showing the aberrant splicing effect of *TXNRD2* c.1348-1G>T (D).

Figure 3. Structural analysis of wild-type (WT) TXNRD2 and mutant p.(Met450Valfs*20). A. Multiple sequence alignment of TXNRD2 homologues across species showed a highly conserved C-terminus. B,C. Analysis of the monomeric forms of WT (B) and mutant structure of TXNRD2 (C). D. Partial structure of p.(Met450Valfs*20) showing several missing residues at the C-terminus of the protein. E. WT TXNRD2 homodimer. F. Visualization of an active site selenocysteine located at the dimer interface of human WT TXNRD2 proteins.

Figure 4: Steroid profiling of patient-derived induced adrenal-like cells (iALC) carrying the *TXNRD2* c.1348-1G>T variant and showing inhibited steroidogenesis. Steroid metabolites secreted into the cell supernatants were measured by LC-MS. A. Pathway view showing concentrations of metabolites comprised in the mineralocorticoid, glucocorticoid, and adrenal androgen paths, respectively. B. Net production of precursor pregnenolone and end products aldosterone, cortisol, and DHEA, Testosterone.

Figure 5: MitoSOX-based flow cytometry assessing mitochondrial ROS/superoxide production of wild-type (WT) control and *TXNRD2* c.1348-1G>T iALC (TXNRD2mut). Representative blots without and with MitoSOX (left and right panel) for WT (A) and mutant TXNRD2 iALC (B). C. Quantification of H_2O_2 production (ROS balancing) activity expressed as % of WT without MitoSOX.

References

1. Flück CE. MECHANISMS IN ENDOCRINOLOGY: Update on pathogenesis of primary adrenal insufficiency: beyond steroid enzyme deficiency and autoimmune adrenal destruction. Eur J Endocrinol. 2017 Sep;177(3):R99–111.

2. Meimaridou E, Hughes CR, Kowalczyk J, Guasti L, Chapple JP, King PJ, et al. Familial glucocorticoid deficiency: New genes and mechanisms. Mol Cell Endocrinol. 2013 May 22;371(1–2):195–200.

3. Maharaj A, Maudhoo A, Chan LF, Novoselova T, Prasad R, Metherell LA, et al. Isolated glucocorticoid deficiency: Genetic causes and animal models. J Steroid Biochem Mol Biol. 2019 May;189:73–80.

4. Prasad R, Kowalczyk JC, Meimaridou E, Storr HL, Metherell LA. Oxidative stress and adrenocortical insufficiency. J Endocrinol. 2014 Jun;221(3):R63-73.

5. Galea E, Launay N, Portero-Otin M, Ruiz M, Pamplona R, Aubourg P, et al. Oxidative stress underlying axonal degeneration in adrenoleukodystrophy: A paradigm for multifactorial neurodegenerative diseases? Biochim Biophys Acta BBA - Mol Basis Dis. 2012 Sep;1822(9):1475–88.

6. Prasad R, Metherell LA, Clark AJ, Storr HL. Deficiency of ALADIN impairs redox homeostasis in human adrenal cells and inhibits steroidogenesis. Endocrinology. 2013 Sep;154(9):3209–18.

7. Meimaridou E, Goldsworthy M, Chortis V, Fragouli E, Foster PA, Arlt W, et al. NNT is a key regulator of adrenal redox homeostasis and steroidogenesis in male mice. J Endocrinol. 2018 Jan;236(1):13–28.

8. Prasad R, Chan LF, Hughes CR, Kaski JP, Kowalczyk JC, Savage MO, et al. Thioredoxin Reductase 2 (TXNRD2) Mutation Associated With Familial Glucocorticoid Deficiency (FGD). J Clin Endocrinol Metab. 2014 Aug 1;99(8):E1556–63.

9. Prasad R, Hadjidemetriou I, Maharaj A, Meimaridou E, Buonocore F, Saleem M, et al. Sphingosine-1-phosphate lyase mutations cause primary adrenal insufficiency and steroid-resistant nephrotic syndrome. J Clin Invest. 2017 Feb 6;127(3):942–53.

10. Corkery-Hayward M, Metherell LA. Adrenal Dysfunction in Mitochondrial Diseases. Int J Mol Sci. 2023 Jan 6;24(2):1126.

11. Lu J, Holmgren A. Thioredoxin system in cell death progression. Antioxid Redox Signal. 2012 Dec 15;17(12):1738–47.

12. Mahmood DFD, Abderrazak A, El Hadri K, Simmet T, Rouis M. The thioredoxin system as a therapeutic target in human health and disease. Antioxid Redox Signal. 2013 Oct 10;19(11):1266–303.

13. Zhang H, Go YM, Jones DP. Mitochondrial thioredoxin-2/peroxiredoxin-3 system functions in parallel with mitochondrial GSH system in protection against oxidative stress. Arch Biochem Biophys. 2007 Sep 1;465(1):119–26.

14. Meimaridou E, Kowalczyk J, Guasti L, Hughes CR, Wagner F, Frommolt P, et al. Mutations in NNT encoding nicotinamide nucleotide transhydrogenase cause familial glucocorticoid deficiency. Nat Genet. 2012 May 27;44(7):740–2.

15. Jazayeri O, Liu X, van Diemen CC, Bakker-van Waarde WM, Sikkema-Raddatz B, Sinke RJ, et al. A novel homozygous insertion and review of published mutations in the NNT gene causing familial glucocorticoid deficiency (FGD). Eur J Med Genet. 2015 Dec;58(12):642–9.

16. Sibbing D, Pfeufer A, Perisic T, Mannes AM, Fritz-Wolf K, Unwin S, et al. Mutations in the mitochondrial thioredoxin reductase gene TXNRD2 cause dilated cardiomyopathy. Eur Heart J. 2011 May;32(9):1121–33.

17. Rajapreyar I, Sinkey R, Pamboukian SV, Tita A. Did a shared thioredoxin-reductase gene mutation lead to maternal peripartum cardiomyopathy and fatal dilated cardiomyopathy in her son? A case report. Case Rep Womens Health. 2020 Apr;26:e00196.

18. Maddirevula S, Alzahrani F, Al-Owain M, Al Muhaizea MA, Kayyali HR, AlHashem A, et al. Autozygome and high throughput confirmation of disease genes candidacy. Genet Med Off J Am Coll Med Genet. 2019 Mar;21(3):736–42.

19. Patjamontri S, Lucas-Herald AK, McMillan M, Prasad R, Metherell LA, McGowan R, et al. Thioredoxin Reductase 2 Variant as a Cause of Micropenis, Undescended Testis, and Selective Glucocorticoid Deficiency. Horm Res Paediatr. 2023 Nov 27;1–6.

20. Holzerova E, Danhauser K, Haack TB, Kremer LS, Melcher M, Ingold I, et al. Human thioredoxin 2 deficiency impairs mitochondrial redox homeostasis and causes early-onset neurodegeneration. Brain. 2016 Feb 1;139(2):346–54.

21. Rebelo AP, Eidhof I, Cintra VP, Guillot-Noel L, Pereira CV, Timmann D, et al. Biallelic loss-of-function variations in PRDX3 cause cerebellar ataxia. Brain J Neurol. 2021 Jun 22;144(5):1467–81.

22. Martínez-Rubio D, Rodríguez-Prieto Á, Sancho P, Navarro-González C, Gorría-Redondo N, Miquel-Leal J, et al. Protein misfolding and clearance in the pathogenesis of a new infantile onset ataxia caused by mutations in PRDX3. Hum Mol Genet. 2022 Nov 10;31(22):3897–913.

23. Santesmasses D, Mariotti M, Gladyshev VN. Tolerance to Selenoprotein Loss Differs between Human and Mouse. Mol Biol Evol. 2020 Feb 1;37(2):341–54.

24. Okita K, Matsumura Y, Sato Y, Okada A, Morizane A, Okamoto S, et al. A more efficient method to generate integration-free human iPS cells. Nat Methods. 2011 May;8(5):409–12.

25. Lee-Montiel FT, Laemmle A, Charwat V, Dumont L, Lee CS, Huebsch N, et al. Integrated Isogenic Human Induced Pluripotent Stem Cell-Based Liver and Heart Microphysiological Systems Predict Unsafe Drug-Drug Interaction. Front Pharmacol. 2021;12:667010.

26. Laemmle A, Poms M, Hsu B, Borsuk M, Rüfenacht V, Robinson J, et al. Aquaporin 9 induction in human iPSC-derived hepatocytes facilitates modeling of ornithine transcarbamylase deficiency. Hepatol Baltim Md. 2022 Sep;76(3):646–59.

27. Li L, Li Y, Sottas C, Culty M, Fan J, Hu Y, et al. Directing differentiation of human induced pluripotent stem cells toward androgen-producing Leydig cells rather than adrenal cells. Proc Natl Acad Sci U S A. 2019 Nov 12;116(46):23274–83.

28. Andrieu T, du Toit T, Vogt B, Mueller MD, Groessl M. Parallel targeted and non-targeted quantitative analysis of steroids in human serum and peritoneal fluid by liquid

chromatography high-resolution mass spectrometry. Anal Bioanal Chem. 2022 Oct;414(25):7461–72.

29. Kauffman M, Kauffman M, Traore K, Zhu H, Trush M, Jia Z, et al. MitoSOX-Based Flow Cytometry for Detecting Mitochondrial ROS. React Oxyg Species [Internet]. 2016 [cited 2024 Mar 27]; Available from: http://www.rosj.org/index.php/ros/article/view/62

30. Biterova EI, Turanov AA, Gladyshev VN, Barycki JJ. Crystal structures of oxidized and reduced mitochondrial thioredoxin reductase provide molecular details of the reaction mechanism. Proc Natl Acad Sci U S A. 2005 Oct 18;102(42):15018–23.

31. Roucher-Boulez F, Mallet-Motak D, Samara-Boustani D, Jilani H, Ladjouze A, Souchon PF, et al. NNT mutations: a cause of primary adrenal insufficiency, oxidative stress and extra-adrenal defects. Eur J Endocrinol. 2016 Jul;175(1):73–84.

32. Hershkovitz E, Arafat M, Loewenthal N, Haim A, Parvari R. Combined adrenal failure and testicular adrenal rest tumor in a patient with nicotinamide nucleotide transhydrogenase deficiency. J Pediatr Endocrinol Metab JPEM. 2015 Sep;28(9–10):1187–90.

33. Miller WL. Steroidogenic electron-transfer factors and their diseases. Ann Pediatr Endocrinol Metab. 2021 Sep;26(3):138–48.

34. Rapoport R, Sklan D, Hanukoglu I. Electron leakage from the adrenal cortex mitochondrial P450scc and P450c11 systems: NADPH and steroid dependence. Arch Biochem Biophys. 1995 Mar 10;317(2):412–6.

35. Soerensen J, Jakupoglu C, Beck H, Förster H, Schmidt J, Schmahl W, et al. The Role of Thioredoxin Reductases in Brain Development. Hatfield DL, editor. PLoS ONE. 2008 Mar 19;3(3):e1813.

1

2 **Table 1.** Reported patients with TXNRD2 variants and their phenotype

Pat	*TXNRD2* Variant		Zygocity	Sex	Age at diagnosis	Age at last visit	Phenotype				Reference
	c.	p.			years	years	**Adrenal**	**Cardiac**	**Neurologic**	**Other**	
1.1	c.1341T>G	p.Y447X	**homo**	f	10.8		**FGD**	normal	nr	nr	Prasad 2014
1.2	c.1341T>G	p.Y447X	**homo**	f	4.5		**FGD**	MR, TR	nr	nr	Prasad 2014
1.3	c.1341T>G	p.Y447X	**homo**	m	2.9		**FGD**	normal	nr	nr	Prasad 2014
1.4	c.1341T>G	p.Y447X	**homo**	f	6.9		**FGD**	normal	nr	nr	Prasad 2014
1.5	c.1341T>G	p.Y447X	**homo**	f	0.1		**FGD**	normal	nr	nr	Prasad 2014
1.6	c.1341T>G	p.Y447X	**homo**	f			Normal	normal	nr	nr	Prasad 2014
1.7	c.1341T>G	p.Y447X	**homo**	m	0.1		**FGD**	TA, VSD	nr	nr	Prasad 2014
2	c.1252C>T	p.R418X	**homo**	m	12		**FGD**	TA, PS	Epilepsy, intellectual disability	Dysmorphic facies, omphalocele	Maddirevula 2018
3	c.1081G>A	p.V361M	**homo**	m	10		**FGD**	normal	nr	Micropenis, cryptorchidism	Patjamontri 2023
4	c.1348-1G>T	p.V450fsX20	homo	m	1.75	17	FGD	normal	PMD, spasticity, optic neuropathy	Micropenis	This report
5	c.175G>A	p.Ala59Thr	het	m	nr	Died at age 68	nr	DCM	nr	nr	Sibbing 2011
6	c.175G>A	p.Ala59Thr	het	m	nr	Died at age 65	nr	DCM	nr	nr	Sibbing 2011
7	c.1124G>A	p.Gly375Arg	het	m	nr	Died at age 83	nr	DCM	nr	nr	Sibbing 2011
8.1	c.1054C>A	p.Pro352Thr	het	f	40	42	nr	DCM	nr	Preeclampsia	Rajapreyar 2020
8.2	c.1054C>A	p.Pro352Thr	het	m	0.1	Died at 0.5	nr	DCM	nr	Multiorgan failure	Rajapreyar 2020

8.3	c.1054C>A	p.Pro352Thr	het	f		Middle aged adult	nr	normal	nr	Healthy	Rajapreyar 2020

Abbreviations:
DCM, dilated cardiomyopathy
FGD, familial glucocorticoid deficiency
GC def, glucocorticoid deficiency
het, heterozygote
homo, homozygote
MR, mitral regurgitation
nr, not reported
PS, pulmonary stenosis
TA, truncus arteriosus
TR, tricuspid regurgitation

Table 2. Laboratory findings of the index case at different ages

	Reference range	Age at laboratory investigation				
		1 day	6 weeks	4 months	21 months	16 years[1)]
ACTH (pg/ml)	7.2-63.3	**-**	**113**	**437**	**2656**	-
Cortisol, basal 8 am (nM)	166-507	270	414	485	**<0,3**	-
Androstenedione (nM)	0.18-0.98*		1	0.2	**<0.1**	-
DHEAS (nM)	30-723*	**<30**	-	**<30**	**<30**	-
Cortisol, ACTH-stimulated (nM)	>450	-	-	742	**<0.3**	-
DHEA, ACTH-stimulated (nM)		-	-	**<0.5**	**<0.5**	-
17OHP, ACTH-stimulated (nM)	<30	-	-	1.81	**<0.2**	-
Androstenedione, ACTH-stimulated (nM)		-	-	2.4	**<0.1**	-
Aldosterone (ng/dl)	5-30	-	-	**42.5**	**-**	-
Plasma Renin Activity (mU/l)	4.4-46	-	-	-	**77**	-
Testosterone (nM)	0.69-7.6 *	**-**	**0**	**0.2**	0	13
Testosterone, hCG-stimulated (nM)	>10 *	**-**	**0.5**	-	-	-
LH (UI/l)	0.6-4 *	-	0.7	0.3	0.7	**16**
FSH (UI/l)	0.4-3 *	-	1.1	1.7	1.9	**39**
Serum Na (mM)	135-145				136	
Serum K (mM)	3.4-4.7				4	
Serum Glucose (mg/dl)	70-100				93	
HbA1c (%)	4-6.5					5.4
Creatine Kinase (UI/l)	29-308					41
Lactate (mM/l)	0.7-2					**2.5**

Notes:
[1)] under hydrocortisone and fludrocortisone supplementation therapy since age 21 months
Values in **bold** are outside the reference range for age.
hCG-stimulation protocol: 1500 Units, 6 injections
*Reference range during mini puberty

1

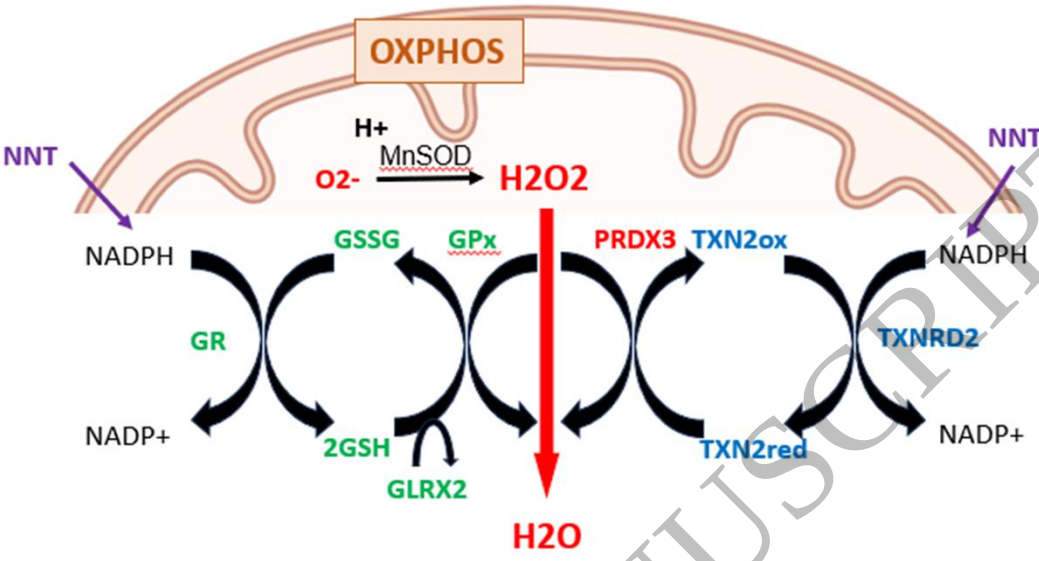

2

3 *Figure 1*
4 *160x88 mm (x DPI)*

5

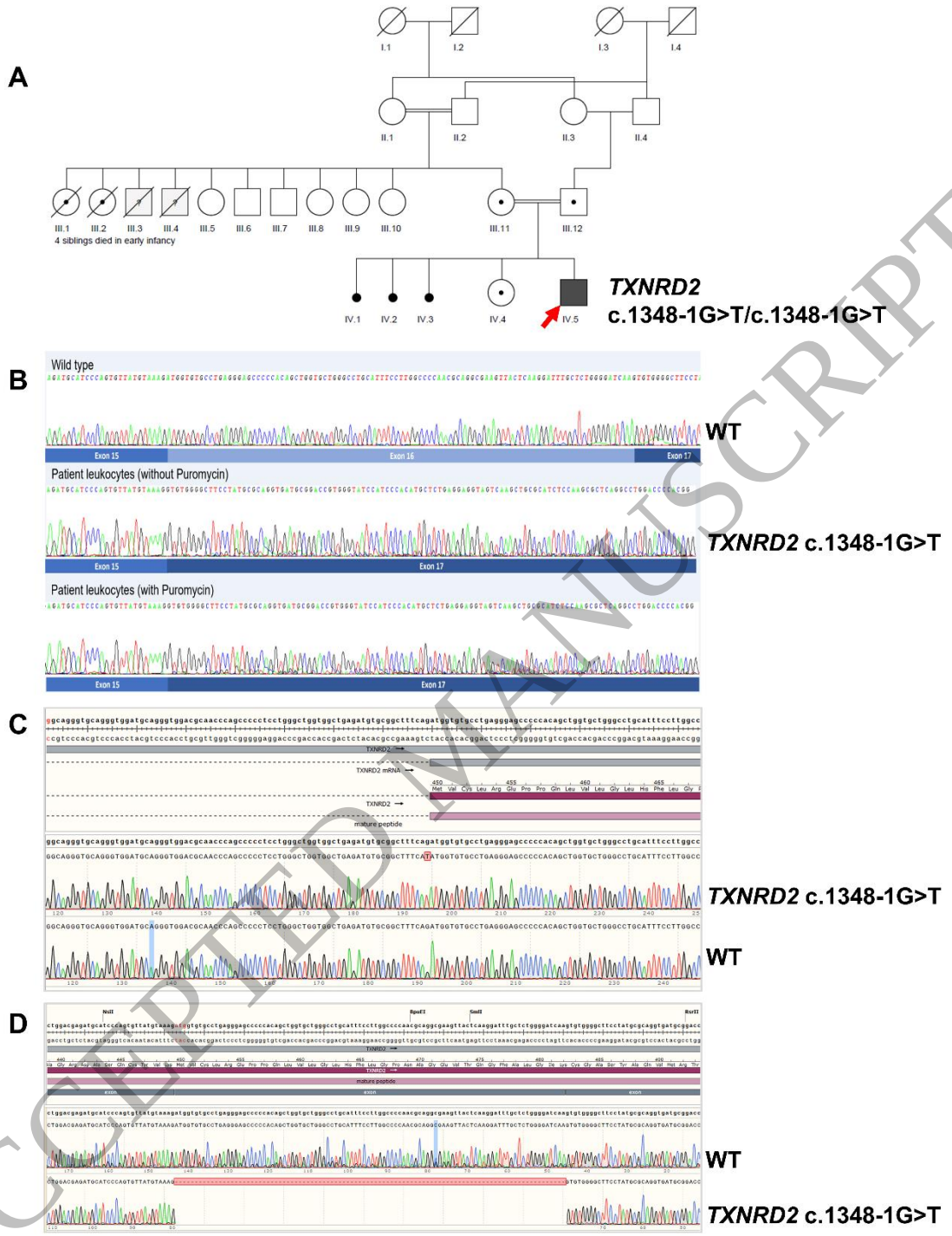

Figure 2
158x198 mm (x DPI)

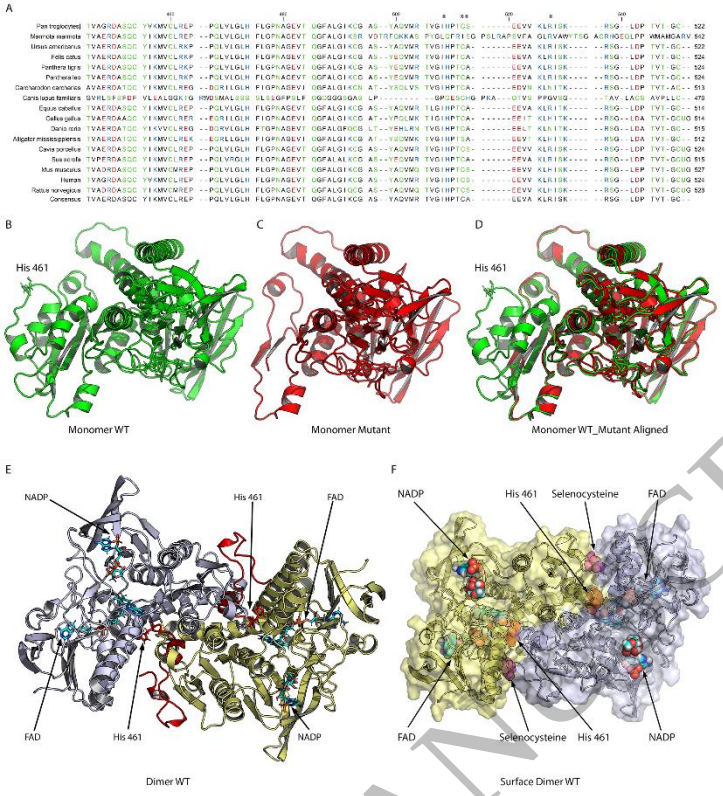

Figure 3
95x107 mm (x DPI)

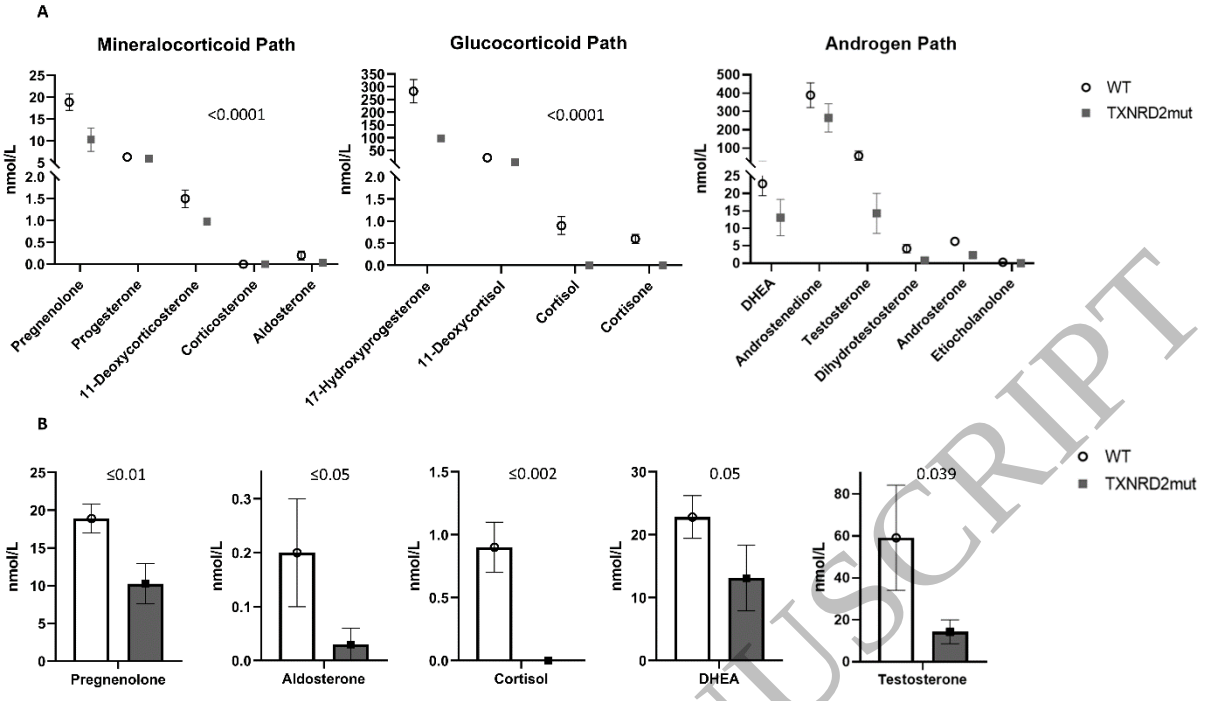

Figure 4
160x93 mm (x DPI)

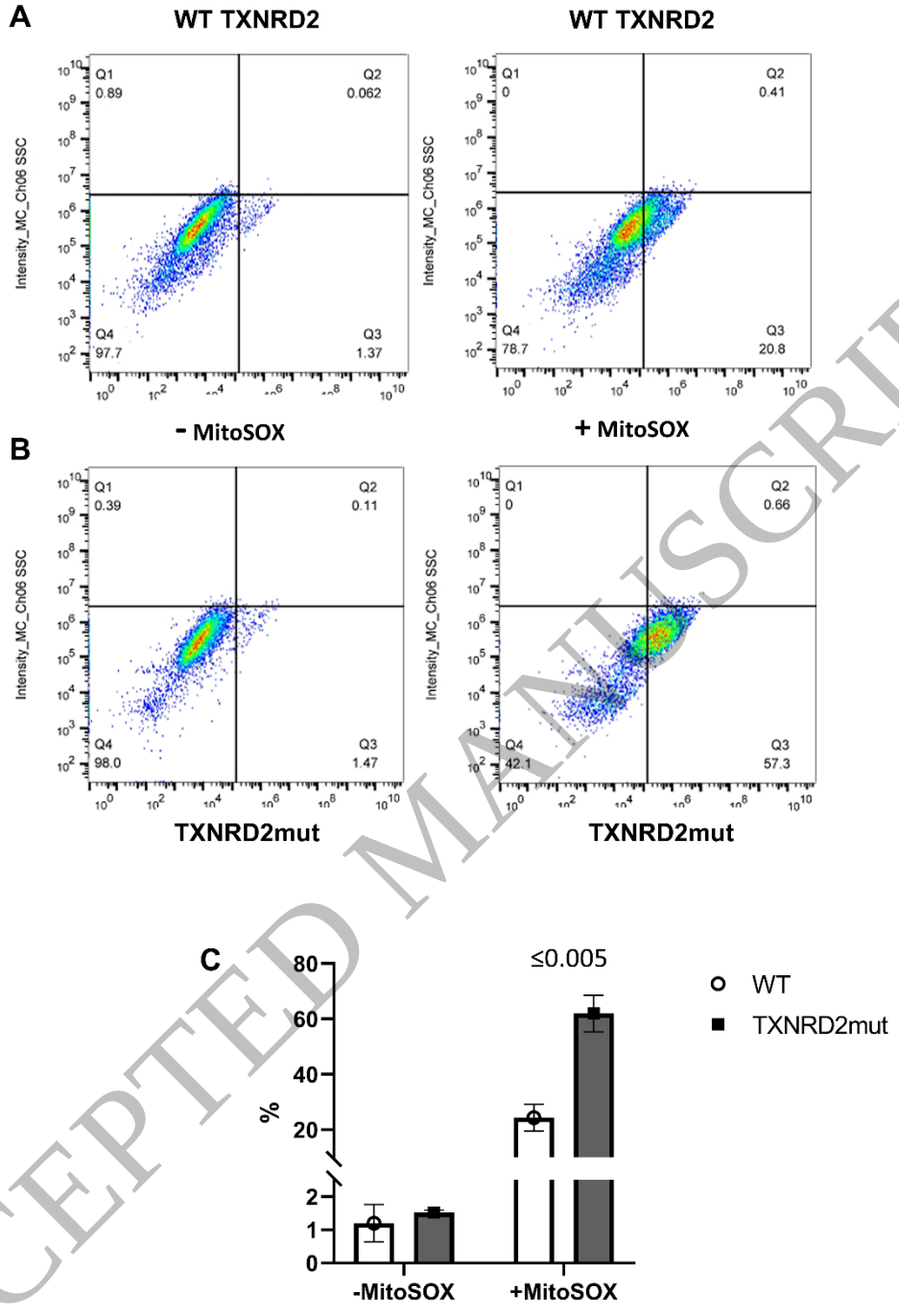

Figure 5
135x186 mm (x DPI)